

Debye relaxation equations for a standard linear solid with high relaxation strength

M. CALLENS-RAADSCHELDERS, R. DE BATIST, R. GEVERS

Materials Science Department, S.C.K./C.E.N., B-2400 Mol, Belgium and Rijksuniversitair Centrum Antwerpen, B-2020, Antwerpen, Belgium

In internal friction measurements, relaxational effects are very often analysed in terms of the classical Debye equations, which are derived for processes with low relaxation strength. In a theoretical study it is shown that, in the case of high relaxation strength processes, deviations from the features of the Debye plots for damping and modulus defect occur. Calculations have been performed as well for the experimental situation of constant frequency as for resonance measurements. Whereas for the former only a shift of the modulus defect with respect to the peak maximum occurs, for the latter an even larger shift of the peak maximum and a narrowing of the peak plotted as a function of relaxation time is observed. Moreover, the influence of a temperature-dependent relaxation strength is studied and seen to yield an asymmetric damping peak when plotted as a function of temperature. Finally, the theoretical results, compared with some experimental observations, are shown to be able to qualitatively explain observed deviations from simple Debye type behaviour.

1. Introduction

Mechanical damping measurements have proved to be able to yield valuable information about the structural properties of both crystalline and amorphous materials. This is so because a large number of energy dissipating mechanisms can be formally described as arising from the stress-induced relaxation of an internal order parameter. Assuming that the rate of approach to equilibrium of this order parameter is proportional to its deviation from its equilibrium value, Zener [1] has shown that the behaviour of such a solid can be described in terms of a fairly simple mechanical model consisting of two Hookean springs and one Newtonian dashpot. This model has been called a standard linear solid by Zener, a standard anelastic solid by Nowick and Berry [2]. It is clear that the constitutive equation for such a solid can be written as a linear combination of stress, strain and their first time derivatives. The solid is then fully characterized by three material constants. One of these parameters is related to the elastic properties of the material, the other two describe its relax-

ational properties. These parameters can be determined experimentally by measuring the strength and the rate of the relaxation effect, either in a static experiment (creep, elastic after-effect, stress relaxation) or in a dynamic one (attenuation, internal friction). Depending upon the kind of experiment used for determining the internal friction, several measures of the damping have been adopted in the literature. In a free decay experiment, the logarithmic decrement, δ , is the logical choice. For a forced vibration experiment, on the other hand, one may use either the width of the resonance peak in terms of the quality factor, i.e. Q^{-1} , the specific amount of energy dissipated each half cycle, $\Delta W/2W$ (vibration absorption engineers use more frequently the specific damping capacity, $\Delta W/W$), or the phase angle, ϕ , between stress and strain. Since the relaxation strength is usually relatively small (often less than 1%), one may use the simple conversion factors between these quantities given in most textbooks:

$$\Delta W/2W = \delta = \pi Q^{-1} = \pi \tan \phi.$$

However, as pointed out by Zener [3] about 30 years ago, this is no longer true when the relaxation strength becomes larger than say 10%. The relationships between the relaxation strength and the various measures used for the specimen damping can still be derived rigorously and so, in principle, the material parameters can still be determined experimentally. But obviously the precision with which a large δ or resonance peak width can be measured cannot be very high and, even more important, when these damping experiments are performed by a resonance-type method, a very large modulus defect is found to occur in the region of large damping. Since the natural variable to be used in describing a relaxation effect in a dynamic experiment is $\omega\tau$, the product of angular frequency and relaxation time, this will clearly induce a change in peak shape with respect to the small damping case.

Consequently, if one wants to investigate a large relaxation strength process by means of a resonance experiment, one will have to use the complete analysis of the behaviour of the standard linear solid, in which the modulus variation due to the relaxation process is fully taken into account. This is actually a blessing in disguise, as this will allow one to determine the material parameters from the shape of the modulus versus relaxation time curve instead of from the peak height. In fact, it was precisely the observation of a relative displacement along the relaxation time axis of a damping peak in PVF₂ and the corresponding modulus defect which induced us to consider in detail the behaviour of a standard linear solid under conditions of large relaxation strength.

In order to make the paper as self-contained as possible, we will first briefly recall the results for the small damping case, leading to the well-known Debye relaxation equations. Next, we will drop the restriction of a small relaxation strength. We then consider successively experiments at constant frequency and resonance-type experiments, either in free decay or under conditions of sustained oscillation. In order to provide a molecular basis for the phenomenological mechanical model description, a very simple two-position model is then introduced. This shows qualitatively how large relaxation strengths may arise physically and how the peak shape versus temperature (which is of course the usual way of collecting experimental results) is influenced by the magnitude of the

relaxation strength. Finally, a comparison is made with a few experimental observations.

2. Classical Debye relations

The constitutive equation for Zener's standard linear solid is written most usefully in the following form:

$$T + \tau_S \dot{T} = M_R S + M_R \tau_T \dot{S} \quad (1)$$

where T is the stress, S the strain, τ_S the relaxation time for the stress at constant strain, τ_T the relaxation time for the strain at constant stress, and M_R the relaxed elastic modulus. It is then easy to show [4] that the unrelaxed modulus M_U is given by

$$M_U = M_R \frac{\tau_T}{\tau_S}. \quad (2)$$

Although stress and strain should, in principle, be used in their tensorial form, it suffices for our purpose to restrict them to their scalar uniaxial expressions, so that also M_U and M_R become scalar quantities.

The definitions given for τ_S and τ_T are evident from a consideration of the solutions of Equation 1 for constant strain S_0 , and constant stress T_0 , respectively:

$$T = M_R S_0 + (T_0 - M_R S_0) e^{-t/\tau_S} \quad (3)$$

$$S = M_R^{-1} T_0 + (S_0 - M_R^{-1} T_0) e^{-t/\tau_T}. \quad (4)$$

It is also clear that stress relaxation (at constant S_0) and creep (at constant T_0) will occur in a standard linear solid only when the relaxed elastic modulus is different from the unrelaxed one. Indeed, when $M_U = M_R$, $T_0 = M_U S_0 = M_R S_0$ and Equations 3 and 4 reduce to $T = M_R S_0 = T_0$. The occurrence of time-dependent effects implies therefore that $\tau_S < \tau_T$ (the relaxed modulus is necessarily smaller than the unrelaxed one).

If instead of a static experiment as described by Equations 3 or 4 one performs a dynamic experiment in which stress and strain vary harmonically with time, anelasticity will manifest itself by a phase difference between stress and strain and hence by a dissipation of mechanical energy.

Making use of the Boltzmann superposition principle, we can restrict the discussion to the first term of a Fourier series of a periodically varying stress and strain:

$$T = T_0 e^{i\omega t} \quad (5a)$$

$$S = S_0 e^{i\omega t}. \quad (5b)$$

The phase-lag between stress and strain is taken account of by the complex quantity S_0 . Hence, a complex modulus:

$$\tilde{M} = \frac{T_0}{S_0} = M_R \frac{1 + i\omega\tau_T}{1 + i\omega\tau_S} \quad (6)$$

can be defined and expressed in terms of the parameters of Equation 1 by substitution of Equation 5 into Equation 1.

This complex modulus consists of a real part, which is called the dynamic modulus M and an imaginary part which is a measure for the damping ϕ [4]. Hence:

$$\tilde{M} = M + iM\phi \quad (7)$$

Equating Equations 6 and 7 for the complex modulus and assuming for the time being $\tau_S/\tau_T \approx 1$, one can introduce geometric averages:

$$\tau = (\tau_S \tau_T)^{1/2} \quad (8a)$$

$$M_0 = (M_U M_R)^{1/2} \quad (8b)$$

and obtain expressions known as the classical Debye relations [4]:

$$\phi = \frac{M_U - M_R}{M_0} \frac{\omega\tau}{1 + (\omega\tau)^2} \quad (9)$$

$$M = M_U - \frac{M_U - M_R}{1 + (\omega\tau)^2}. \quad (10)$$

Plotted as a function of $\ln(\omega\tau)$ a maximum for ϕ and a maximum for the variation of M occur at $\omega\tau = 1$.

3. Debye relations for arbitrary relaxation strength

The effect of a large relaxation strength on the relation between the various damping measures in a resonance type experiment has been studied by Zener [3] through a combination of the equation of motion of a vibrating solid with the constitutive equation for a standard linear solid. Whereas Zener gave only the results for the peak damping values, Parke [5] also considered the resulting changes in peak shape. Neither of these authors, however, has considered in detail the behaviour of the modulus defect and the information to be derived from the modulus versus relaxation time relationship. As a matter of fact, the usefulness of modulus measurements in the case of a large relaxation strength

standard linear solid can be demonstrated most easily for constant frequency experiments. These will therefore be discussed first.

3.1. Measurements at constant frequency

As already stated, the classical Debye relations are deduced by assuming $\tau_S \approx \tau_T$. In cases of a large relaxation strength, however, this approximation is no longer valid and the expressions for damping and modulus defect become (cf. e.g. [7]):

$$\phi = \frac{M_U - M_R}{M_0} \frac{\omega\tau}{1 + (\omega\tau)^2} \quad (9)$$

$$M = M_U - \frac{M_U - M_R}{1 + (\tau_S/\tau_T)(\omega\tau)^2}. \quad (11)$$

One notices that the expression for the damping remains the same as for small relaxation strength. Hence, the maximum of the damping peak still occurs for $\omega\tau = 1$. In order to investigate the shift of the modulus defect with respect to the damping peak, one introduces a new parameter:

$$\eta = \frac{M(\omega\tau \gg 1) - M(\omega\tau = 1)}{M(\omega\tau = 1) - M(\omega\tau \ll 1)} \quad (12)$$

Using Equation 11, this gives immediately:

$$\eta = \frac{\tau_T}{\tau_S} \quad (13)$$

From Equation 11, the inflection point for the modulus as a function of $\ln(\omega\tau_S)$, occurs at $\omega\tau_S = 1$. Since $\tau_S < \tau$, this inflection point lies at the high τ -value side of the damping peak (or at the low temperature side for a relaxation process which is thermally activated).

This result then allows one to determine the values of the two relaxation times τ_S and τ_T from the experimentally determined modulus values. The ratio τ_T/τ_S can be obtained from the ratio M_U/M_R of the modulus values on either side of the relaxation peak. The value of τ_S can be obtained from the position of the inflection point or, alternatively, the value of $\tau_S\tau_T$ can be obtained from the damping peak position occurring at the point where the ratio of the two modulus defect fractions η is equal to τ_T/τ_S .

Instead of using a constant frequency, one may profitably use resonance experiments in which the modulus is related directly to the observed resonance frequency of the solid. This is discussed in the next section.

3.2. Resonance measurements

When a resonance method is used for measuring damping and modulus, the specimen is allowed to oscillate in one of its mechanical resonance modes. The resonance frequency is then determined by the geometry of the specimen, the kind of vibration mode and the elastic and anelastic properties of the material (modulus and damping).

This means that the ω , appearing in the Debye relations, is itself a function of the damping and the modulus. Provided the relaxation strength is rather low, ω can be considered approximately as a constant. However, when a large modulus defect occurs (as a function of τ or of temperature), the resonance frequency changes considerably. In the derivation of the Debye relations we now have to take account of the dependence of ω on modulus and damping, and therefore we have to introduce the equation of motion of the system under consideration.

In the following we consider two possible experimental methods: the free decay and the forced resonance. The equation of motion for these two cases can be written, assuming that no anharmonic effects occur, i.e. that the oscillation is amplitude independent, as:

$$m\ddot{S} + \tilde{M}S = 0 \quad \text{for free decay} \quad (14)$$

$$= P_0 e^{i\omega t} \quad \text{for forced resonance} \quad (15)$$

where \tilde{M} is a complex modulus, describing the elastic and anelastic properties, m is a measure of inertia and $P_0 e^{i\omega t}$ is an external driving force.

3.2.1. Implicit expressions

3.2.1.1. *Free decay.* A solution of the equation of motion (Equation 14) is:

$$S = S_0 e^{i\omega^* t} \quad (16)$$

where ω^* is a complex frequency given by:

$$\omega^{*2} = \frac{\tilde{M}}{m}. \quad (17)$$

An expression for the stress is then given by:

$$T = T_0 e^{i\omega^* t} \quad (18)$$

where T_0/S_0 is complex in order to take account of the phase-lag between stress and strain due to anelastic effects. Substituting these expressions for S and T into the standard linear solid equation of Zener (Equation 1), one obtains an expression for the complex modulus \tilde{M} as a function of the

resonance frequency, the relaxed modulus and the relaxation times:

$$\tilde{M} = M_R \frac{1 + i\omega^* \tau_T}{1 + i\omega^* \tau_S}. \quad (19)$$

Assuming that the specimen is homogeneous and that its behaviour is strain amplitude independent, one can equate both expressions (Equations 17 and 19) for the complex modulus. Hence:

$$M_R \frac{1 + i\omega^* \tau_T}{1 + i\omega^* \tau_S} = m\omega^{*2}. \quad (20)$$

Putting $\omega^* = \omega [1 + i(\delta/2\pi)]$, where δ is the logarithmic decrement [4], one can separate the real and imaginary parts in Equation 20:

$$2\omega^2 \frac{\delta}{2\pi} = \frac{M_R}{m} \frac{\omega(\tau_T - \tau_S)}{[1 - \omega\tau_S(\delta/2\pi)]^2 + \omega^2\tau_S^2} \quad (21)$$

and:

$$\omega^2 \left[1 - \left(\frac{\delta}{2\pi} \right)^2 \right] = \frac{M_R}{m} \frac{\left(1 - \omega \frac{\delta}{2\pi} \tau_S \right) \left(1 - \omega \frac{\delta}{2\pi} \tau_T \right) + \omega^2 \tau_S \tau_T}{\left(1 - \omega \tau_S \frac{\delta}{2\pi} \right)^2 + \omega^2 \tau_S^2}. \quad (22)$$

Rewritten in terms of new variables:

$$y = \frac{\delta}{2\pi}, \quad (23)$$

$$x = \omega\tau = \omega\sqrt{\tau_S\tau_T} \quad (24)$$

and

$$\gamma^2 = \frac{\tau_T}{\tau_S}, \quad (25)$$

Equations 21 and 22 can be combined to yield implicit expressions for $\delta/2\pi$ and for ω^2 :

$$\frac{2y}{1-y^2} = \frac{x \left(\gamma - \frac{1}{\gamma} \right)}{1 + x^2 - yx \left(\gamma + \frac{1}{\gamma} \right) + y^2 x^2} \quad (26)$$

$$\omega^2 = \frac{M_R}{m} \frac{(1 - \gamma xy) \left(1 - \frac{1}{\gamma} xy \right) + x^2}{\left(1 - \frac{1}{\gamma} xy \right)^2 + (1/\gamma^2)x^2} \cdot \frac{1}{1-y^2}. \quad (27)$$

One notices that for small values of y Equation 26 reduces to the classical Debye relation (Equation 9), namely:

$$2y = \frac{x[\gamma - (1/\gamma)]}{1 + x^2} \quad (28)$$

In this case, the peak maximum

$$y' = 0 \quad \text{appears for} \quad x = 1 \quad (29)$$

and the associated peak height is given by:

$$y_{\max} = \frac{\gamma - (1/\gamma)}{4}. \quad (30)$$

Let us now consider the corrections appearing in the case of high damping. Equation 26 can be written as:

$$F(x, y) = 2x^2y^3 - \left(\gamma + \frac{3}{\gamma}\right)xy^2 + 2(1 + x^2)y - \left(\gamma - \frac{1}{\gamma}\right)x = 0. \quad (31)$$

The condition for the peak maximum $y' = 0$, can then be written as:

$$\frac{\partial F}{\partial x} = 0 \quad (32)$$

Hence:

$$4xy^3 - \left(\gamma + \frac{3}{\gamma}\right)y^2 + 4xy - \left(\gamma - \frac{1}{\gamma}\right) = 0. \quad (33)$$

Equations 31 and 33 form a set of two equations, which can be written as:

$$2(1 + x^2)y - \left(\gamma - \frac{1}{\gamma}\right)x = -2x^2y^3 + \left(\gamma + \frac{3}{\gamma}\right)xy^2 = -a \quad (34)$$

$$4xy - \left(\gamma - \frac{1}{\gamma}\right) = -4xy^3 + \left(\gamma + \frac{3}{\gamma}\right)y^2 = -b \quad (35)$$

where a and b depend on x and on higher powers of y and hence are correction terms. Furthermore the x and y values satisfying Equations 34 and 35 correspond to the peak maximum and can be represented as x_M and y_M . One calculates easily:

$$x_M = \left[\frac{\gamma - (1/\gamma) - b}{\gamma - (1/\gamma) + b} + \left(\frac{a}{\gamma - (1/\gamma) + b} \right)^2 \right]^{1/2} + \frac{a}{\gamma - (1/\gamma) + b} \quad (36)$$

$$y_M = \frac{\gamma - (1/\gamma) - b}{4x_M} \quad (37)$$

Since the parameter η , which was introduced by means of Equation 12, is a good measure for the relaxation strength in the case of high damping in non-resonance cases (Section 3.1), we must also derive an expression for it in the case of resonance measurements. In this last case the frequency is used as a measure for the modulus [4]. Therefore, the expression for η will now be based on the fact that the modulus is proportional to the square of the frequency:

$$\eta = \frac{\omega_{x \rightarrow \infty}^2 - \omega_{x_M}^2}{\omega_{x_M}^2 - \omega_{x \rightarrow 0}^2} = \frac{\gamma^2 - \frac{(1 - \gamma xy)[1 - (1/\gamma)xy] + x^2}{[1 - (1/\gamma)xy]^2 + (1/\gamma^2)x^2} \frac{1}{1 - y^2}}{\frac{(1 - \gamma xy)[1 - (1/\gamma)xy] + x^2}{[1 - (1/\gamma)xy]^2 + (1/\gamma^2)x^2} \frac{1}{1 - y^2} - 1} \quad (38)$$

where $x = x_M$ and $y = y_M$. For small relaxation strength ($y_M \ll 1, x_M = 1$):

$$\eta = \gamma^2$$

which corresponds with Equation 13.

In Fig. 1 we have plotted the relative variation of the parameters η , x_M and y_M as a function of γ^2 . Relative means here the ratio of the correct

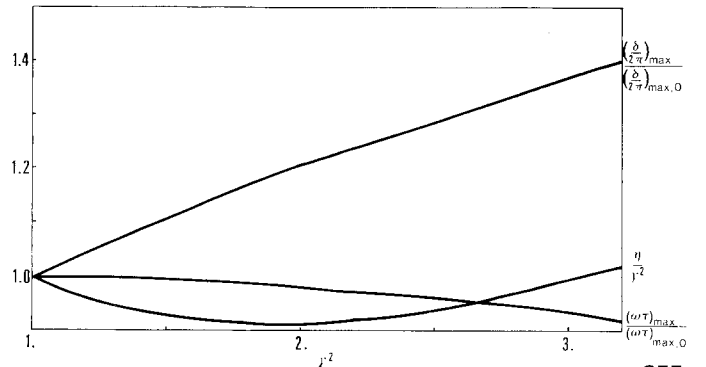


Figure 1 Free decay: ratio of the exact expressions for $(\delta/2\pi)_{\max}$, $(\omega\tau)_{\max}$ and η (Equations 37, 36, 38) to the extrapolated relations valid at small damping (Equations 30, 29, 13) as a function of $\gamma^2 = \tau_T/\tau_S$. The index 0 refers to the case $a = b = 0$.

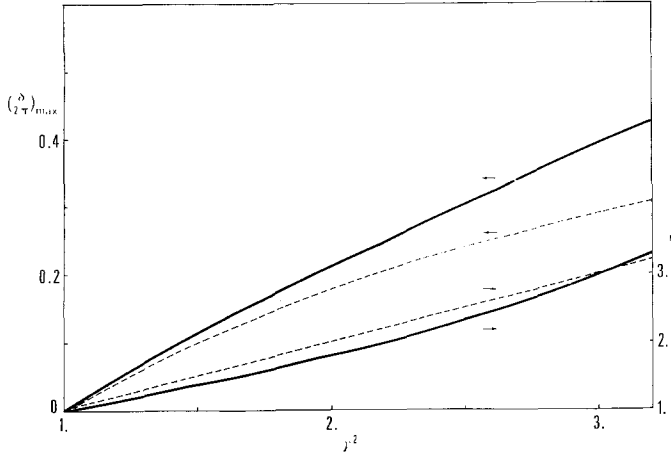


Figure 2 Free decay: the solid lines give exact values of $(\delta/2\pi)_{\max}$ and η , the broken lines give extrapolated low damping values.

values of the parameters (Equations 38, 36, 37), against the values calculated from the expressions for low damping (Equations 13 and 25, 29, 30). The exact values of x_M and y_M are determined from Equations 36 and 37 by means of an iteration method, in which initial values for x_M and y_M are obtained for $a = b = 0$ and Equations 34 and 35 are used for determining new values for a and b .

From Fig. 1 one derives the magnitude of the relative error made by using the classical Debye relations in the case of high damping free decay measurements. In Fig. 2 the absolute values of y_M and η are plotted as a function of γ^2 . This figure gives the possibility of determining graphically the value of $\tau_T/\tau_S = \gamma^2$ from experimental values of peak height or η . Since the value of $[\sqrt{(\omega^2 \tau_S \tau_T)}]_M$ associated with the thus obtained γ^2 can be found in Fig. 1, τ_T and τ_S can again be calculated separately.

3.2.1.2. *Forced resonance.* A solution for the equation of motion (Equation 15) can be written as:

$$S = S_0 e^{i(\omega t - \varphi)} \quad (39)$$

where ω is a real frequency and φ denotes the phase-lag which appears between driving force and strain. For the stress one has:

$$T = T_0 e^{i(\omega t - \varphi)} \quad (40)$$

where T_0/S_0 is complex and can be written in terms of the Zener relation:

$$\frac{T_0}{S_0} = \tilde{M} = M_R \frac{1 + i\omega\tau_T}{1 + i\omega\tau_S} \quad (41)$$

The damping is measured by means of the ratio $\Delta W/W$, in which $\Delta W = \int_0^{2\pi} T dS$ is the energy

dissipated during one stress cycle and $W = \int_0^{\pi/2} T dS - \Delta W/4$ is the maximum potential energy [2]. Hence:

$$\frac{1}{\pi} \frac{\Delta W}{2W} = \frac{M_U - M_R}{M_0} \frac{\omega\tau}{1 + \omega^2\tau^2} \quad (42)$$

One notices that this expression does not differ from the classical Debye relation. The peak maximum always occurs at $\omega\tau = 1$ and the peak height is equal to

$$\Delta W/2\pi W = (\gamma - 1/\gamma)/4 \quad (43)$$

just as derived from the classical Debye relations.

In order to calculate the resonance frequency, one derives an expression for the strain amplitude by substitution of Equations 39 and 41 in the equation of motion (Equation 15):

$$-m\omega^2 S_0 + M_R \frac{1 + i\omega\tau_T}{1 + i\omega\tau_S} S_0 = P_0 e^{i\varphi} \quad (44)$$

Hence:

$$|S_0|^2 = \frac{P_0^2 (1 + \omega^2 \tau_S^2)^2}{[M_R \omega (\tau_T - \tau_S)]^2 + [M_R (1 + \omega^2 \tau_S \tau_T) - m \omega^2 (1 + \omega^2 \tau_S^2)]^2} \quad (45)$$

Expressing the condition for resonance gives:

$$\begin{aligned} & \omega^2 \tau^2 \left(\omega^4 \frac{M_R}{M_U} - \omega^2 \frac{M_R}{m} \right) \\ & + \left(2\omega^4 - 2\omega^2 \frac{M_U}{m} + \frac{M_U^2}{2m^2} - \frac{M_R^2}{2m^2} \right) \\ & + \frac{1}{\omega^2 \tau^2} \left(\omega^4 \frac{M_U}{M_R} - \omega^2 \frac{M_U}{m} \right) = 0. \quad (46) \end{aligned}$$

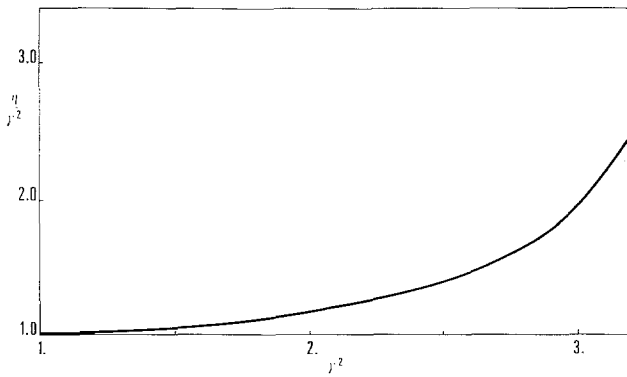


Figure 3 Forced resonance: ratio of the exact expression for η (Equation 49) to the extrapolated relation valid at small damping (Equation 13) as a function of $\gamma^2 = \tau_T/\tau_S$.

One notices that for $\omega\tau \gg 1$

$$\omega^2 = \frac{M_U}{m} \quad (47a)$$

and for $\omega\tau \ll 1$

$$\omega^2 = \frac{M_R}{m} \quad (47b)$$

In order to obtain an expression for

$$\eta = \frac{\omega_{x \rightarrow \infty}^2 - \omega_{x=1}^2}{\omega_{x=1}^2 - \omega_{x \rightarrow 0}^2}$$

with

$$x = \omega\tau \quad (24)$$

one first calculates $\omega^2(x=1)$:

$$\omega_{x=1}^2 = \frac{M_R}{m} \times \frac{(1 + 3\gamma^2) + \sqrt{\{5 + 6\gamma^2 + 5\gamma^4 + 2[(1/\gamma^2) - \gamma^6]\}}}{2[(1/\gamma^2) + \gamma^2 + 2]} \quad (48)$$

For η one can then write:

$$\eta = \gamma^2 \frac{(1 + 3\gamma^2) + \sqrt{\{5 + 6\gamma^2 + 5\gamma^4 + 2[(1/\gamma^2) - \gamma^6]\}}}{2[(1/\gamma^2) + \gamma^2 + 2]} \frac{(1 + 3\gamma^2) + \sqrt{\{5 + 6\gamma^2 + 5\gamma^4 + 2[(1/\gamma^2) - \gamma^6]\}}}{2[(1/\gamma^2) + \gamma^2 + 2]} - 1 \quad (49)$$

In Figs. 3 and 4 we plot the relative and absolute variation of the parameter η as a function of γ^2 . One notices that the deviation of η from the extrapolated low damping value γ^2 is much larger in the case of forced resonance than for free decay (cf. Figs. 2 and 4). The relaxation times τ_S and τ_T can again be calculated from Fig. 4 and from the relation $\sqrt{(\tau_S\tau_T)} = 1/\omega$, which is valid at the peak maximum.

3.2.2. Explicit expressions

In addition to the relationships concerning the peak maximum, one may also consider the effect of large relaxation strength on the entire peak shape.

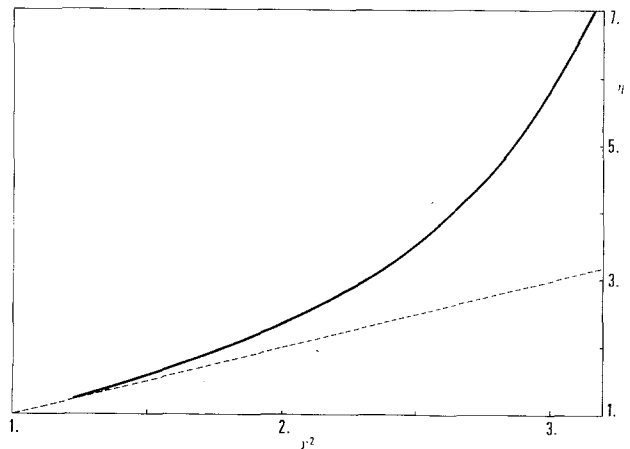


Figure 4 Forced resonance: the solid line gives exact value of η , the broken line gives extrapolated low damping value.

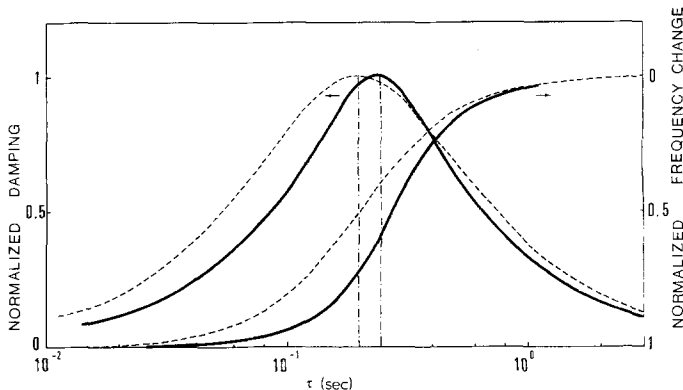


Figure 5 Free decay: normalized damping, δ/δ_{\max} , and normalized change in frequency, $(\omega_{\tau \rightarrow \infty} - \omega_{\tau})/(\omega_{\tau \rightarrow \infty} - \omega_{\tau \rightarrow 0})$, as a function of average relaxation time for a relaxation strength of $M_R/M_U = 0.999$ giving a $\delta_{\max} = 1.57 \times 10^3$ (broken line) and $M_R/M_U = 0.5$ giving a $\delta_{\max} = 1.32$ (solid line). The resonance frequency for high τ -values has been chosen arbitrarily equal to 5 Hz for both cases.

3.2.2.1. *Free decay.* Instead of deriving the implicit Equations 26 and 27, one derives from Equation 20 a set of two equations in the two unknowns δ and ω as functions of τ . Taking Equations 23, 24, 25, 2 and 8a into account one gets:

$$3\omega^2 y^2 - 2 \frac{\omega}{\tau} \gamma y + \frac{M_U}{m} - \omega^2 = 0 \quad (50)$$

$$\omega^3 (y^3 - 3y) + \frac{\omega^2}{\tau} \gamma (1 - y^2) + \frac{M_U}{m} \omega y - \frac{M_U}{m} \frac{1}{\tau} \frac{1}{\gamma} = 0. \quad (51)$$

In Fig. 5 a numerical example has been plotted for two different orders of magnitude of the relaxation strength ($\tau_S/\tau_T = M_R/M_U = 0.999$ and 0.5) and for a given value of the unrelaxed modulus ($M_U/m = 25 \text{ Hz}^2$).

The unknowns δ and ω have been calculated as a function of the parameter τ by solving the set of two equations with the help of a computer-programmed iteration method. Since the properties of the peak maximum have been discussed in the previous section in terms of the implicit relations, we will here only consider character-

istics of the entire peak shape and the modulus defect. As one notices from Fig. 5 the half-width of the damping peak plotted as a function of $\ln \tau$, is smaller for the high damping case. One also notices a shift in the modulus defect to higher τ -values. This will be discussed in more detail in Section 3.2.2.2.

3.2.2.2. *Forced resonance.* An explicit expression for the damping and frequency is already given by Equations 42 and 46. In Fig. 6 a numerical example has been plotted for two different orders of magnitude of the relaxation strength ($M_R/M_U = \tau_S/\tau_T = 0.999$ and 0.5) and for a given value of the unrelaxed modulus ($M_U/m = 25 \text{ Hz}^2$). The calculations are done with the help of a computer program. One notices that again the high damping peak has the smallest half-width.

Another interesting property, which can be visualized in Fig. 6, is the shift of the modulus defect with respect to the peak maximum. We know that for low damping the symmetry point of the modulus defect lies near the peak maximum position. In terms of the parameter η introduced in Equation 12 as the ratio of the parts into which the modulus defect is divided by the peak position

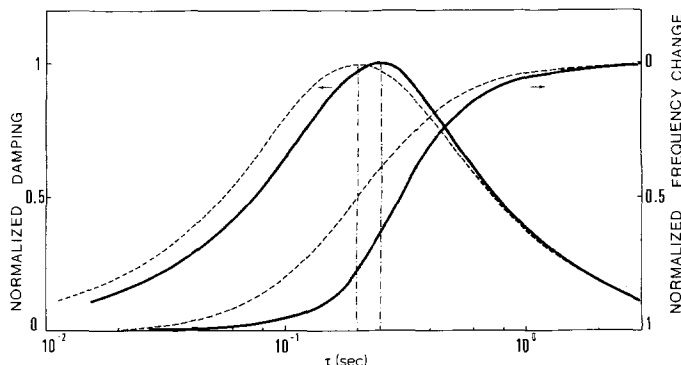


Figure 6 Forced resonance: as Fig. 5 with $(\Delta W/2W)_{\max} = 1.57 \cdot 10^{-3}$ and $(\Delta W/2W)_{\max} = 1.11$ respectively.

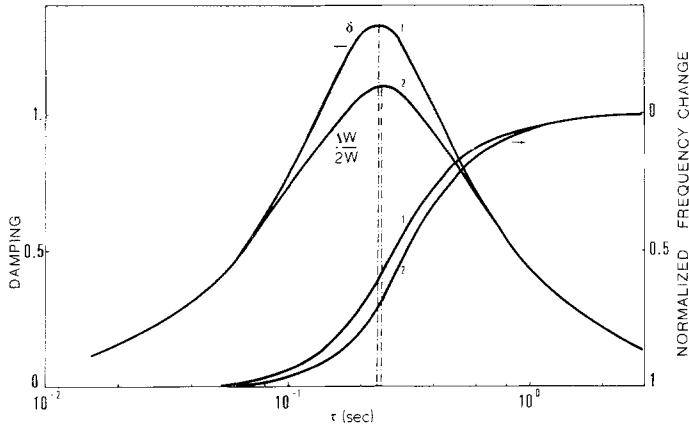


Figure 7 Damping and normalized change in frequency for a relaxation process with a relaxation strength $M_R/M_U = 0.5$ measured in free decay (1) and forced resonance (2). The resonance frequency for high τ -values has been chosen equal to 5 Hz.

this means that for low damping $\eta \approx 1$. For larger values of the damping this value of η increases, which means that the modulus defect shifts to the high τ value side (or low temperature side). One may notice that this shift also occurs in the case of non-resonance measurements (see Section 3.1). However, this shift effect is very pronounced in the case of forced resonance since the value of η increases much more rapidly than $\gamma^2 = \tau_T/\tau_S$, which is proportional to the relaxation strength. This important shift of the modulus defect can also be noticed in Fig. 7 where we plotted for comparison the modulus defect and damping for the same relaxation strength in free decay and forced resonance. This plot also shows that δ_{\max} and $(\Delta W/2W)_{\max}$ have a different value in case of high damping. This can also be deduced from Equations 43 and 37 and Fig. 2.

4. Relaxation due to stress-induced thermally activated internal ordering

The constitutive equation for the standard linear solid can be derived in a phenomenological way by introducing a parameter describing the state of internal order of the solid and by making a number of assumptions about the stress dependence of this parameter and about its rate of approach to its equilibrium value [3]. The Zener standard linear solid can also be given an atomistic foundation by considering the thermodynamics of a specific molecular species incorporated in the solid and causing a change in free energy of the solid when it is acted upon by an external field (e.g. [2, 4]). Anelasticity then results if this molecular species can occupy in the solid a number of equivalent positions which can be made non-equivalent in the presence of an external field and if these equilibrium positions are separated by

energy barriers so that the attainment of equilibrium is delayed. In the simplest atomistic model for a Zener solid, one considers a species which can occupy one of two equilibrium positions characterized by a Gibbs free energy level γ_0 in the absence of external stress, γ_1 or γ_2 when a stress T is applied to the solid. The free energy of the solid when the species is at the saddle point between the two equilibrium positions is H_0 when $T = 0$ and H_1 when $T \neq 0$.

The stress-induced change in the free energy level is determined by the change in strain S_m generated by reorientation of the molecular species:

$$S_{m,i} = V\lambda_i \left(N_i - \frac{N}{2} \right) \quad (52)$$

($i = 1$ or 2 , N_i is the population of position i , $N = N_1 + N_2$ is the total population and V is the molecular volume). Restricting oneself to the linear approximation, one may then write:

$$\gamma_i = \gamma_0 - V\lambda_i T \quad (i = 1 \text{ or } 2) \quad (53)$$

$$H_1 = H_0 + \alpha T. \quad (54)$$

This is represented in the schematic free energy diagram of Fig. 8.

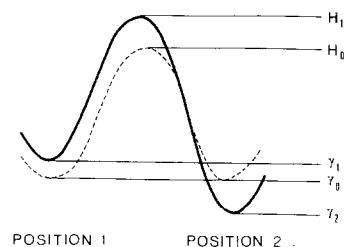


Figure 8 Schematic free energy diagram for a simple two position model.

The transition probabilities w_{12} and w_{21} between positions 1 and 2 can then be written as:

$$w_{12} = w_{21} = w_0 \exp\left[-\frac{H_0 - \gamma_0}{k\theta}\right] = w \quad \text{for } T = 0 \quad (55)$$

$$w_{12} = w_0 \exp\left[-\frac{H_1 - \gamma_1}{k\theta}\right] \quad (56)$$

and

$$w_{21} = w_0 \exp\left[-\frac{H_1 - \gamma_2}{k\theta}\right] \text{ for } T \neq 0, \quad (57)$$

(k is Boltzmann's constant and θ the absolute temperature). The rate equation for the population N_1 is then:

$$\dot{N}_1 = -N_1 (w_{12} + w_{21}) + N w_{21}. \quad (58)$$

The constitutive equation follows from the expression for the strain, S :

$$S = \frac{T}{M_U} + S_{m,1} + S_{m,2} = \frac{T}{M_U} + V(\lambda_1 - \lambda_2) \left(N_1 - \frac{N}{2}\right) \quad (59)$$

which relates N_1 to T and S .

Hence:

$$\dot{S} = \frac{\dot{T}}{M_U} + V(\lambda_1 - \lambda_2) \dot{N}_1 \quad (60)$$

and:

$$M_U \dot{S} + M_U (w_{12} + w_{21}) S = \dot{T} + (w_{12} + w_{21}) T + M_U \frac{N}{2} V(\lambda_1 - \lambda_2) (w_{21} - w_{12}) \quad (61)$$

in which w_{12} and w_{21} are still functions of T .

For sufficiently small stresses, $\alpha T \ll k\theta$ and $\lambda_i T \ll k\theta$ and one may linearize the stress dependence of the transition probabilities so that*:

$$w_{21} - w_{12} \simeq V(\lambda_1 - \lambda_2) \frac{wT}{k\theta}. \quad (62)$$

Hence:

$$S + \frac{1}{w_{12} + w_{21}} \dot{S} = \frac{1}{w_{12} + w_{21}} \frac{\dot{T}}{M_U} + T \left[\frac{1}{M_U} + \frac{V^2 N}{2} (\lambda_1 - \lambda_2)^2 \frac{w}{w_{12} + w_{21}} \frac{1}{k\theta} \right]. \quad (63)$$

This is equivalent with the Zener equation:

$$S + \tau_T \dot{S} = \frac{1}{M_R} (T + \tau_S \dot{T}) \quad (64)$$

when the parameters τ_T , τ_S and M_R are interpreted as follows:

$$T = (w_{12} + w_{21})^{-1} \simeq \frac{1}{2w} \left(1 + \frac{\alpha T}{k\theta} + \frac{\lambda_1 + \lambda_2}{2k\theta} VT \right) \quad (65)$$

$$\frac{1}{M_R} = \frac{1}{M_U} + \frac{V^2 N (\lambda_1 - \lambda_2)^2 w}{2k\theta (w_{12} + w_{21})} \simeq \frac{1}{M_U} + \frac{V^2 N (\lambda_1 - \lambda_2)^2}{4k\theta \{ 1 - (\alpha T/k\theta) - [(\lambda_1 + \lambda_2)/2k\theta] T \}} \quad (66)$$

$$\tau_S = \frac{M_R}{M_U} \tau_T; \quad (2)$$

It thus appears that τ_T is in general a function of the stress level and becomes independent of T only when $\alpha = -(\lambda_1 + \lambda_2)/2$. Of course, as long as $\alpha T \ll k\theta$ and $\lambda_i T \ll k\theta$, the error made in taking $\tau_T = 1/(2w)$ irrespective of the stress level remains small and this is the point of view usually adopted [2]. On the other hand, the ratio $\gamma^2 = \tau_T/\tau_S = M_U/M_R$ is a function of the temperature θ as well as of the parameters N and $(\lambda_1 - \lambda_2)^2$ which characterize the relaxing molecular species in the solid. Since the magnitude of $(\lambda_1 - \lambda_2)$ is usually only a fraction of unity, it is clear that a large relaxation strength can only be expected for processes in which a large number of molecules take part, i.e. in which VN becomes comparable with one. This brings us to amorphous materials or to materials in which phase transformations occur (although in this latter case the applicability of the simple-minded Zener model becomes questionable).

As pointed out before, the natural variable for the representation of a relaxation effect described by a standard linear solid model is $\omega\tau$, which reduces to τ both for a constant frequency experiment and for a resonance type experiment for which ω can be expressed in terms of τ . For thermally activated processes as discussed here, τ is a function of temperature and experimentally

* For larger stresses, or for small temperatures, this approximation is no longer allowed and Equation 61 cannot be transformed into the standard linear solid shape. The damping peak shape now becomes amplitude-dependent.

one measures the temperature dependence of damping and modulus defect instead of the relaxation time dependence. As a matter of fact, this can be done for any process for which τ depends on temperature (e.g. tunnelling of point defects between equilibrium positions, glass transitions in amorphous polymers, . . .). Therefore, in order to evaluate a relaxation effect one often studies the peak shape in a curve of damping versus temperature.

Since γ^2 is inversely proportional with temperature, one might expect changes in peak shape for large relaxation strengths. In order to estimate this influence, let us consider M_R^{-1} to be a linear function of θ^{-1} :

$$M_R^{-1} = M_U^{-1} + C_1 + C_2\theta^{-1} \quad (C_1 \text{ and } C_2 \text{ are constants}) \quad (67)$$

or:

$$\gamma^2 = \frac{\tau_T}{\tau_S} = \frac{M_U}{M_R} = \frac{\theta + \theta_0}{A\theta} \quad (68)$$

which covers the cases of a temperature-independent relaxation strength ($\theta_0 = 0$) and of a relaxation strength proportional with θ^{-1} ($A = 1$; $\theta_0 = C_2 M_U$). Introducing this temperature-dependent γ into the constitutive equation for the standard linear solid and restricting oneself to a constant frequency experiment as in Section 3.1. yields the following expression for the damping:

$$\phi = \frac{x(\gamma^2 - 1)}{\gamma(1 + x^2)} \quad (69)$$

Taking account of the temperature dependence of $x = \omega\tau = \omega\tau_0 \exp(q/\theta)$ as derived from Equations

55 and 65, one finds that the maximum value ϕ_M of ϕ occurs when:

$$x^2 = x_M^2 = 1 + \frac{2\theta\theta_0(1 + \gamma^2)}{2q(\theta + \theta_0)(\gamma^2 - 1) - \theta\theta_0(1 + \gamma^2)} \equiv 1 + \beta \quad (70)$$

and is given by:

$$\phi_M = \frac{\gamma^2 - 1}{\gamma} \frac{\sqrt{(1 + \beta)}}{2 + \beta} \quad (71)$$

The peak shape can be characterized by the temperatures θ_1 and θ_2 for which $\phi = \frac{1}{2}\phi_M$. This occurs for $x = x_{1,2}$ given by:

$$x_{1,2} = (1 + \beta)^{-1/2} [2 + \beta \pm (3 + 3\beta + \beta^2)^{1/2}] \quad (72)$$

In terms of θ_1 , θ_2 and the peak temperature, θ_M , this yields:

$$\exp q \left(\frac{1}{\theta_1} - \frac{1}{\theta_M} \right) = \frac{x_1}{x_M} = \quad (73)$$

$$[2 + \beta_1 + (3 + 3\beta_1 + \beta_1^2)^{1/2}] [(1 + \beta_M)(1 + \beta_1)]^{-1/2}$$

$$\exp q \left(\frac{1}{\theta_M} - \frac{1}{\theta_2} \right) = \frac{x_M}{x_2} = \quad (74)$$

$$[2 + \beta_2 - (3 + 3\beta_2 + \beta_2^2)^{1/2}]^{-1} [(1 + \beta_M)(1 + \beta_2)]^{1/2}$$

in which β_1 , β_2 and β_M are the values of β for temperatures θ_1 , θ_2 and θ_M , respectively. For reasonable values of q , γ and θ_0 , it appears that

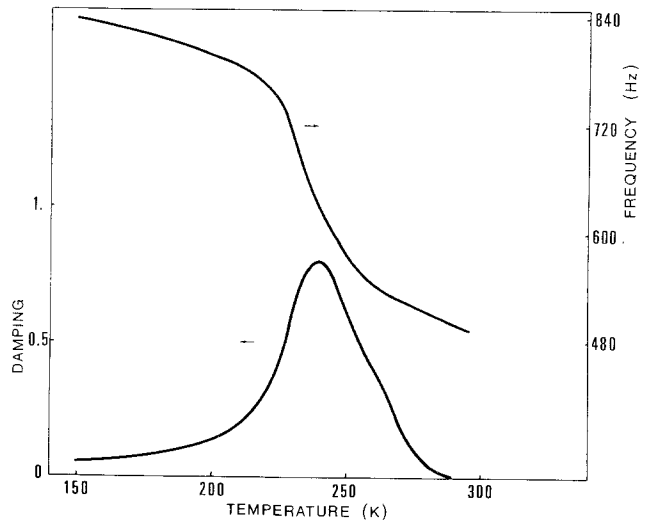


Figure 9 Experimental internal friction results for PVF₂ measured with the forced resonance method [8].

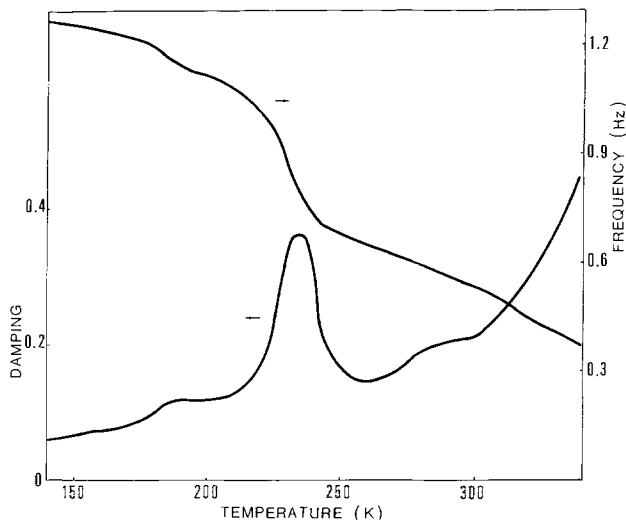


Figure 10 Experimental internal friction results for PVF₂ measured with the free decay method [6].

one may assume $\beta \ll 1$ and approximate the half peak widths in terms of temperature by the following expressions:

$$q \frac{\theta_M - \theta_1}{\theta_1 \theta_M} = 1.317 - \frac{\beta_M}{2} \quad (75)$$

$$q \frac{\theta_2 - \theta_M}{\theta_2 \theta_M} = 1.317 + \frac{\beta_M}{2} \quad (76)$$

This means that the total peak width remains independent of the relaxation strength, as was already found in Section 3.1, where the damping was expressed in terms of $\omega\tau$. However, when the peak is plotted as a function of θ^{-1} instead of as a function of $\ln(\omega\tau)$, it becomes asymmetrical with respect to the peak maximum.

For a resonance type experiment, the peak, when plotted as a function of $\ln(\omega\tau)$, becomes narrower with increasing γ , and one might expect that this change in peak shape adds to the asymmetry derived here for the temperature dependence.

5. Comparison with experimental results

In Figs. 9 and 10 internal friction results (damping and resonance frequency) are plotted as a function of temperature for commercial PVF₂ (polyvinylidene fluoride), measured during forced (Fig. 9) and free (Fig. 10) resonance oscillation [6, 8].

The measurements in forced oscillation are done by means of a transverse resonance method for frequencies of a few hundred Hz. The free decay measurements are performed in a torsion pendulum with frequencies of about 1 Hz.

A relaxation peak with high relaxation strength is noticed in both cases. From the change in frequency one calculates: $M_R/M_U = (540)^2/(800)^2 = 0.46$ in the case of forced resonance and $M_R/M_U = (0.65)^2/(1.09)^2 = 0.36$ in the case of free decay with a damping maximum of respectively 0.8 and 0.38.

In both figures (9 and 10) one observes the shift of the modulus defect symmetry point to lower temperatures with respect to the position of the peak maximum. In terms of the interrelation between relaxation time and temperature (see e.g. [7]) the theoretical results (Figs. 5 to 7) explain the experimental results (Figs. 9 and 10). Indeed, the observed temperature shifts are in the same sense as the calculated time shifts, since time is equivalent with inverse temperature. A quantitative comparison is difficult to make, since this would require a precise knowledge about the time-temperature interrelation existing in the material.

Other experimental results, which show properties predicted by our theoretical study are the high damping measurements on Cu-Al alloys by Koiwa *et al.* [9]. A specific feature of the highest damping peaks (with $\delta = 0.2$) is their narrowness, compared with a single Debye relaxation peak. Koiwa *et al.* argued that this might be due to the fact that in the calculation of the theoretical curve, a constant value of the frequency of vibration is used over the whole range of temperature. Therefore, they plot a corrected curve, taking account of the change of frequency, and find a peak about 4% narrower than the classical Debye peak, but nevertheless still much broader

than their experimental results, for which the half-width is about 40% smaller than the uncorrected theoretical curve. The authors therefore conclude that another reason must be found for the narrowness of the peak. However, the correction, performed by Koiwa *et al.* taking account of the changes in frequency, is only a partial correction since the calculation is, as we presume, still based on the classical Debye equation (Equation 9).

Using our theoretical equations (Equations 50 and 51), we calculated another corrected curve with a relaxation strength deduced from the fall in the frequency. The half-width which follows from our corrected curve is still broader than the experimental results but, being 20% narrower than the Debye peak, lies nearer to them than the 4% narrower peak of Koiwa *et al.* Again, we conclude that our theoretical results can explain the experimental results in a qualitative way, whereas a quantitative comparison is difficult.

Acknowledgement

We are pleased to thank F. Bosmans from the

department of Applied Mathematics of S.C.K. for his assistance concerning programming problems.

References

1. C. M. ZENER, "Elasticity and anelasticity of metals" (University of Chicago Press, Chicago, 1948)
2. A. S. NOWICK and B. S. BERRY, "Anelastic relaxation in crystalline solids", edited by A.M. Alper, J.L. Malgrave and A.S. Nowick (Academic Press, New York and London, 1972).
3. C.M. ZENER, *J. Appl. Phys.* **18** (1947) 1022.
4. R. DE BATIST, "Internal friction of structural defects in crystalline solids" edited by S. Amelinckx, R. Gevers and J. Nihoul (North-Holland, Amsterdam, 1972).
5. S. PARKE, *Brit. J. Appl. Phys.* **17** (1966) 271.
6. A. CALLENS, R. DE BATIST and L. EERSELS, *Nuovo Cimento* **33B** (1976) 434.
7. I. M. WARD, "Mechanical properties of solid polymers" (Interscience, London 1971).
8. A. CALLENS, unpublished results.
9. M. KOIWA, T. ONOZUKA and M. HIRABAYASHI, *Phil. Mag.* **32** (1975) 441.

Received 5 May and accepted 10 June 1976.